Devitrification of Amorphous Celecoxib

Submitted: October 28, 2004; Accepted: March 10, 2005; Published: September 30, 2005

Piyush Gupta,[1] and Arvind K. Bansal[1]

[1]Department of Pharmaceutical Technology (Formulations), National Institute of Pharmaceutical Education and Research (NIPER), S.A.S. Nagar, Punjab 160 062, India

ABSTRACT

The purpose of this research was to analyze the devitrification of amorphous celecoxib (CEL) in the presence of different stressors (temperature, pressure, and/or humidity) encountered during processing of solid dosage forms. Amorphous CEL was prepared in situ in the analytical instruments, as well as in laboratory, by quench-cooling of melt process, and analyzed by dynamic mechanical thermal analysis, differential scanning calorimetry, microscopy, and Fourier-transform infrared spectroscopy. Amorphous CEL prepared in situ in the analytical instruments was resistant to crystallization under the influence of temperature and/or pressure, because of its protection from the external environment during preparation. These samples exhibited structural relaxation during annealing at 25°C/0% relative humidity (RH) for 16 hours. Generation of amorphous CEL in the laboratory resulted in partially crystalline samples, because of exposure to environmental temperature and humidity, resulting in incomplete vitrification. Subjection to thermal stress favored crystallization of amorphous CEL into metastable polymorphic forms, which were not obtained by solvent recrystallization approach. Temperature and humidity were identified as the major factors promoting devitrification of amorphous CEL, leading to loss of solubility advantage. Exposure to International Conference on Harmonization-specified accelerated stability storage conditions (40°C/75% RH) resulted in complete devitrification of amorphous CEL within 15 days. The phase-transformation process of amorphous CEL along the temperature scale was examined visually, as well as spectrally. This propensity for devitrification of amorphous CEL seemed to depend on the strength of differential molecular interactions between the amorphous and crystalline form.

KEYWORDS: amorphous, crystallization, processing, stress, celecoxib

Corresponding Author: Arvind K. Bansal, Department of Pharmaceutical Technology (Formulations), National Institute of Pharmaceutical Education and Research, Sector 67, S.A.S. Nagar, Punjab 160 062, India. Tel: +91-172-2214682-87; Fax: +91-172-2214692; E-mail: akbansal@niper.ac.in

INTRODUCTION

Amorphous state is characterized by randomly arranged molecules, of which the motions are kinetically frozen, at least on experimental time scales.[1] A little provocation by different stressors can accelerate the mobility of molecules and facilitate the achievement of most stable and ordered crystalline states. These issues gain greater importance during pharmaceutical manufacturing processes, wherein a solid experiences the variable extent of stress.

Crystalline and amorphous states of a solid exhibit altered molecular interactions,[2] which may pose as energy barriers for phase transformations. These structural changes depend on adjustment in the nearest-neighbor relationships, including parameters such as intermolecular distances and patterns in hydrogen bonding.[3] The process can be envisioned as a decrease in configurational entropy with a simultaneous increase in the number of molecules constituting cooperatively rearranging regions, favoring a gain of molecular order.

Very few published reports[3-6] had correlated the impact of solid-state alteration during processing on their performance. Stability of the amorphous state is a major hurdle in the successful exploitation of their physicochemical advantage. This stability is additionally challenged in the presence of various processing (temperature; pressure; radiation; and exposure to liquids, gases, and liquid vapors) and performance (humidity) stresses.[4] An understanding of behavior of the altered molecular interaction will help in devising "science-based" strategies for their stabilization.

Quench-cooling of melt of crystalline form resulted in the generation of amorphous celecoxib (CEL).[7] A moderately fragile behavior[8] signified the extent of metastability of this disordered state. Amorphous CEL exhibited high-molecular mobility,[9] even on storage below glass transition temperature (T_g). The solubility advantage from this high-energy form was short-termed because of rapid, water-assisted rearrangement of CEL molecules to form an ordered crystalline lattice.[7] Stabilization of amorphous form was conferred by poly(vinyl pyrrolidone), which reduced the mobility of CEL molecules[9] and provided a solubility advantage.[10]

The present study investigates the impact of different stresses, like temperature, pressure, and/or humidity, on the devitrification process of amorphous CEL. These processing stresses were simulated in different forms, and the

results correlated with actual possibilities. A comprehensive investigation of response of amorphous form to these stressors would provide an in-depth understanding of its tendency for crystallization and strategies for preventing the same.

MATERIALS AND METHODS

The crystalline form of CEL was purchased from Unichem Laboratories Ltd (Maharashtra, India).

Preparation of Amorphous CEL

Amorphous CEL in the laboratory was prepared by melting the crystalline drug in a stainless steel beaker over a hot plate (approximately 175°C) and quench cooling over crushed ice. The chemical stability of the quench-cooled product was assessed by high-performance liquid chromatography, wherein the peak purity was >99.99%.

Dynamic Mechanical Thermal Analysis

The concomitant effect of thermal and mechanical stress on the response of crystalline and amorphous CEL was assessed using dynamic mechanical analyzer (Tritec 2000, Triton Technology Ltd, Nottinghamshire, United Kingdom). Initially, the response of the crystalline sample was recorded. At the end of measurement, the sample holder containing molten drug was quench-cooled by dipping in liquid nitrogen that resulted in the generation of amorphous CEL. The same analytical procedure was then used to study the response of the amorphous sample.

About 100 mg of crystalline CEL was loaded in a sample holder, placed in a single cantilever bending mode, and exposed to oscillating force at 1 Hz with displacement of 0.05 mm. The storage (E') and loss (E'') moduli were recorded in the temperature range of 22 to 180°C with an underlying ramp rate of 5°C/min.

Differential Scanning Calorimetry

The calorimetric response of different samples was measured using differential scanning calorimeter (DSC 821^e, Mettler-Toledo GmbH, Schwerzenbach, Switzerland), operating with STAR^e software version 5.1, and equipped with an intracooler. The samples (3 to 5 mg) were analyzed under dry nitrogen purge (80 mL/min) in sealed and pinholed aluminum pans at a heating rate of 5°C/min, unless otherwise specified. The instrument was calibrated for temperature and heat flow using high-purity standards of 4-nitro toluene, indium, and zinc. Preparation of amorphous CEL in situ in the DSC instrument involved sealing a weighed amount of crystalline CEL in a pin-holed aluminum pan, heating to 175°C at a heating rate of 20°C/min, holding at 175°C for 2 minutes, and then immediately cooling to 25°C at −20°C/min. The T_g has been reported as midvalue of glass transition event, T_c as onset crystallization temperature, and T_m as peak melting temperature.

Microscopy

Optical microscopy was performed using polarized light microscope (DM LP, Leica Microsystems Wetzlar GmbH, Wetzlar, Germany). Hot-stage microscopy was conducted using Leica LMV hot stage. Photographs were acquired using Leica DC 300 camera and analyzed using Leica IM50, version 1.20 release 19, image manager software.

Fourier-Transform Infrared Spectroscopy

The infra-red spectral response of different samples were recorded on a Fourier-transform infrared spectroscopy (FTIR) multiscope spectrometer (Perkin Elmer, Buckinghamshire, United Kingdom) equipped with spectrum v3.02 software, by the conventional KBr pellet method.

The effect of increase in temperature on spectral absorptions were studied using Micro-Press microscope compression cell (CIC Photonics, Inc, Albuquerque, NM), attached with a temperature controller, 1/16 Deutsche Industrial Norms microprocessor-based auto-tuning control, series 965 (Waltow Controls, Winona, MN). The spectral response of crystalline and amorphous CEL was recorded as a function of temperature (5°C/min) in the range 30 to 170°C at intervals of 10°C.

RESULTS AND DISCUSSION

The different stressors were studied individually or in combination to assess their impact on the devitrification tendency of amorphous CEL.

Effect of Mechanical Stress Supplemented With Thermal Stress

During dynamic mechanical thermal analysis (DMTA), an increase in temperature for crystalline CEL showed constant E' values, until a gradual fall at 169°C (Figure 1), signifying the melting of the drug sample. On the other hand, amorphous CEL showed a sharp decline in E' value at 69°C (Figure 1), with minimal changes thereafter. This decrease in E' value for amorphous CEL can be correlated to initiation of cooperative molecular motions, characteristic of the glass transition region.[11] Glass transition is a dynamic event resulting from concordance in measurement frequency to the characteristic frequency of the cooperative rearrangements. The value of tan δ (ratio of E'' and E')[12] is sensitive to molecular mobility and, thus, can be used to

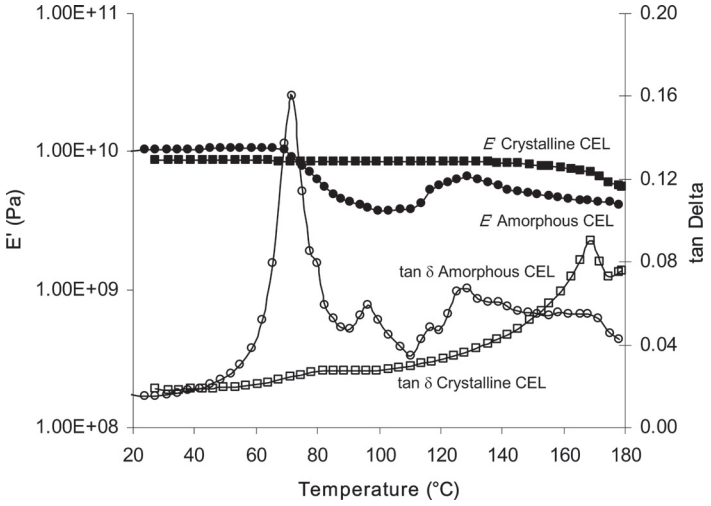

Figure 1. Comparative DMTA response of crystalline and amorphous CEL.

characterize the T_g of amorphous solids.[13] The T_g value was found to be 72°C (the temperature corresponding with maxima in tan δ value). Thus, the simultaneous impact of sinusoidal mechanical force and thermal stress could favor the structural relaxation of amorphous CEL, without extending it to crystallization.

The presently observed T_g value was higher than those noted previously[7-9] for amorphous CEL. Because the transition to liquid state is a relaxation process and is under kinetic control, the glass transition does not, therefore, occur at a specific temperature, but rather over a broad temperature range.[14] Hence, great caution should be taken when comparing the T_g obtained from different analytical methods.[15] The higher T_g value determined by DMTA than by DSC is because of the difference in the principles of these analytical techniques,[16] which measure different properties of the material under study and show variation in relative signal change during determination of this kinetic event. Measurement of T_g by DSC is the result of variation in heat capacity (relative signal change at T_g is 0.2), whereas DMTA measures changes in mechanical strength and energy loss (relative signal change at T_g is 200).[17] This 1,000-fold difference in the measurement signal is responsible for higher T_g values from DMTA measurements. Previous reports[18,19] also indicated the differences between the calorimetric T_g (determined by DSC) and the thermomechanical T_g (determined by DMTA).

Effect of Thermal Stress

As reported earlier,[9] the heating rescan of amorphous CEL prepared in situ in the DSC instrument showed a single thermal transition representing a glass transition event. Thus, exposure of amorphous CEL to thermal stress allowed relaxation of molecules to change their conformation and enter the supercooled liquid region. At T_g, there is a sharp increase in heat capacity[8] because of a greater degree of freedom in the supercooled liquid region facilitating translational motions, in addition to vibrational and rotational motions seen in glassy, as well as crystalline phases.

Motions in randomly arranged molecules in glassy state allow them to interact in a diverse manner with neighboring molecules. During physical aging of a glass, cooperative motions of disordered molecules increase, and this molecular relaxation favors the formation of ordered network on time scales depending on the kinetics of molecular motions.[20] The dynamics of molecular motions for amorphous CEL were assessed in terms of enthalpy lost during annealing of samples at 25°C/0% relative humidity (RH).[9] The relaxation enthalpy for amorphous CEL increased with increasing aging time in a nonlinear fashion. Even up to 16 hours of annealing at these storage conditions, no crystallization was observed in relaxing samples. This implies that aging of amorphous CEL resulted in progression toward relaxed structure but without sufficient mobility to induce crystallization.

DSC analysis of crystalline CEL showed a single sharp melting endotherm in the temperature range of 161.4 to 164.4°C (ΔH_m = 93.8 J/g). On the other hand, amorphous CEL prepared in the laboratory exhibited a glass transition event (58.1°C) followed by recrystallization exotherm in the temperature range of 96.3 to 102.0°C (ΔH_c = 53.5 J/g) and a broad melting endotherm in the temperature range of 161.1 to 168.6°C (ΔH_m = 86.8 J/g). These differences in the thermal response of glassy CEL prepared in situ in the DSC instrument and in the laboratory can be attributed partially to the crystalline nature of the latter because of relatively inferior cooling of the melt and exposure to atmospheric temperature and humidity conditions during preparation, leading to crystallization during DSC analysis. Thus, exposure to thermal stress favored complete devitrification of partially crystalline sample of amorphous CEL.

The melting endotherm of amorphous CEL showed a typical shouldering, which was resolved by DSC analysis at lower heating rates, that is, 1°C/min (Figure 2). The melting endotherm got split into the following 3 sharp endotherms: (1) 157.5 to 158.4°C (ΔH_m = 0.4 J/g), (2) 160.6 to 162.1°C (ΔH_m = 8.8 J/g), and (3) 163.8 to 164.9°C (ΔH_m = 77.2 J/g), which were in close agreement with those reported earlier as forms I, II, and III.[21] Metastable forms often crystallize from solution, but when left in the solvent, they dissolve and crystallize as the least-soluble, most-stable form. Although alternate polymorphic forms of CEL could not be crystallized by conventional solvent recrystallization approach,[7] these endothermic responses indicated the polymorphic forms generated by thermally induced

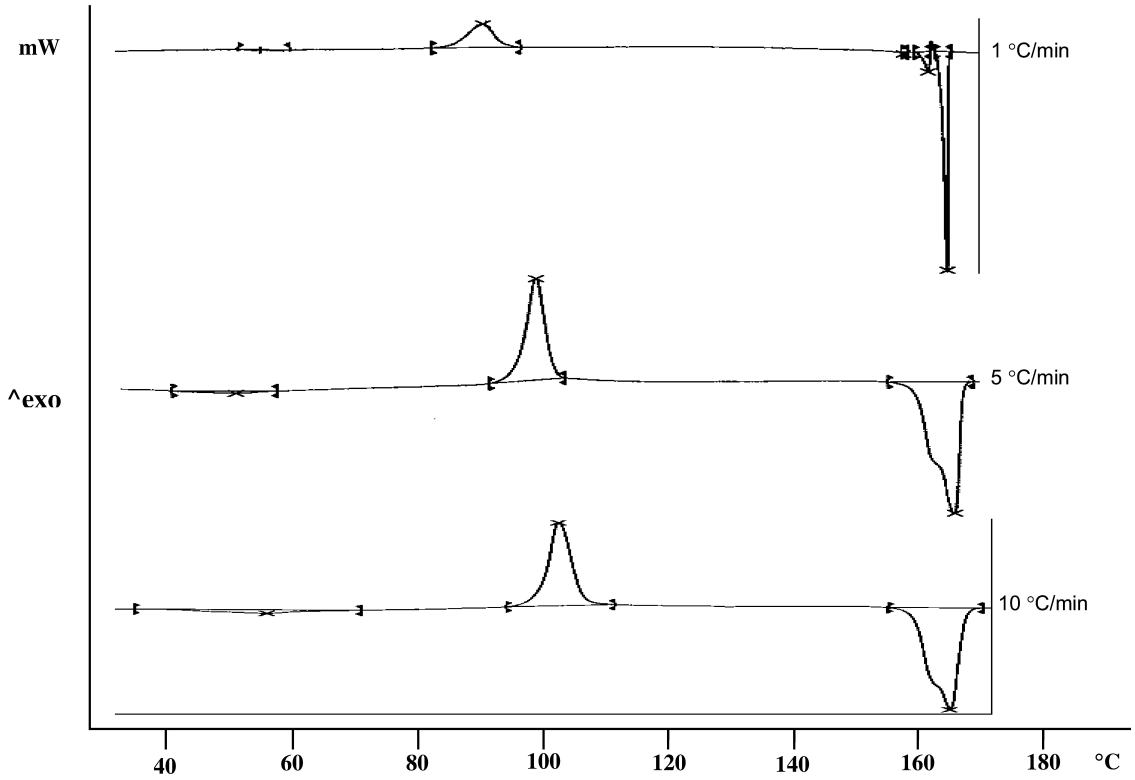

Figure 2. DSC thermograms of amorphous CEL at different heating rates.

recrystallization of amorphous CEL. The presently observed behavior can be correlated with Ostwald's law of stages[22] regarding greater degrees of freedom in a disordered state favoring crystallization into metastable polymorphic forms.

The dynamics of devitrification for amorphous CEL were additionally recapitulated by visualizing these thermal transitions using hot-stage microscopy. In the case of crystalline CEL, the solid sample was found to melt and appear as droplets in the temperature region 160 to 165°C. On the other hand, amorphous CEL (Figure 3) showed origination of needles on edges of amorphous particles (surface crystallization) at 100°C, formation of rosettes with various needles arranged in a circle with common center (bulk crystallization) at 102°C, followed by transformation to melt droplets at around 165 to 170°C. Thus, amorphous CEL exhibited thermally induced crystallization.

Vibrational spectroscopy offers the possibility of gaining a molecular-level view (possibly H-bond interactions) of the macroscopic changes that occur in crystalline and amorphous materials as they are heated.[23] On heating, as T_g is approached, the specific volume begins to increase more rapidly because of a larger thermal expansion coefficient in the liquid than in the glassy state, which has a similar behavior to that for the crystalline state.[24] These volume differences affect intermolecular distances and, hence, intermolecular interactions. As reported previously,[7] the FTIR analysis of crystalline CEL showed *N*-H stretching vibration as a sharp doublet at 3,338 and 3,232 cm^{-1}, and S = O asymmetric stretching vibration at 1,347 cm^{-1}. Amorphous CEL showed shifts to 3,367 and 3,264 cm^{-1} for *N*-H stretching vibration and 1,339 cm^{-1} for S = O asymmetric stretching vibration. The recording of FTIR spectra as a function of temperature facilitated the coupling

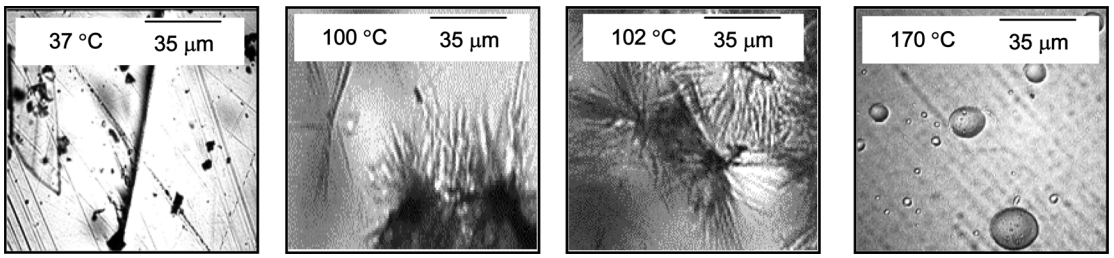

Figure 3. Hot-stage photomicrographs for amorphous CEL.

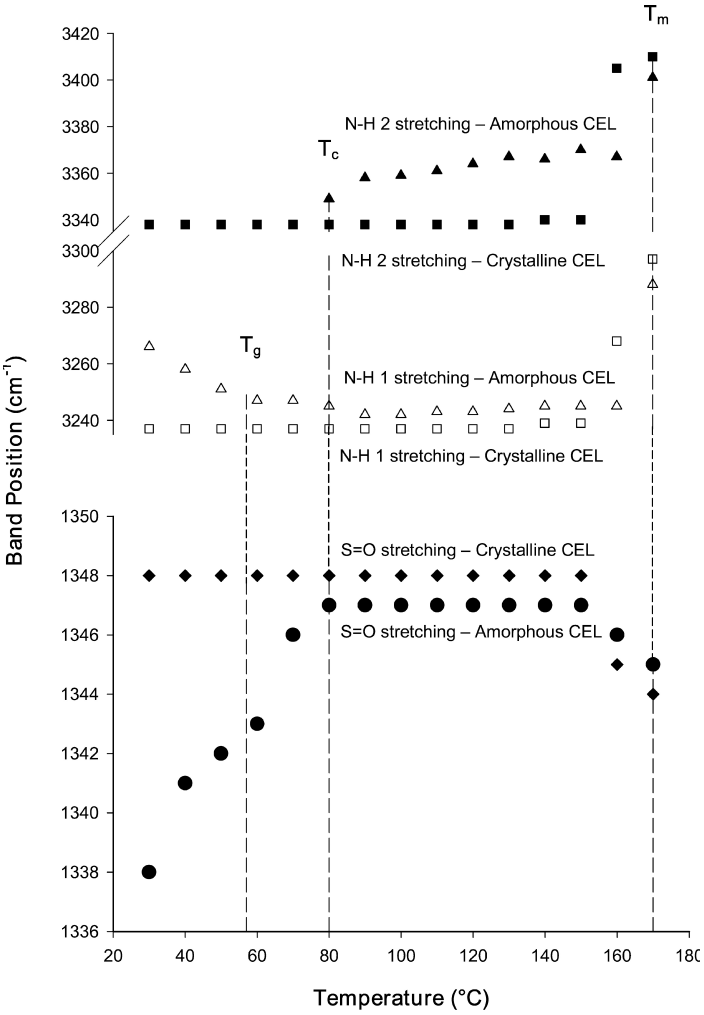

Figure 4. Wave number vs. temperature plot for *N*-H and S = O stretching vibration bands of crystalline and amorphous CEL.

of thermal and spectral responses of amorphous CEL as it progressed through glass transition, supercooled liquid, and, finally, liquid (melt) region.

An increase in temperature resulted in minimal variations in FTIR band positions for crystalline CEL, except for shift to higher wave numbers for *N*-H stretching (Figure 4) and lower wave number for S = O asymmetric stretching (Figure 4) vibration bands near 160°C, which marks the onset of the melting phenomenon. On the other hand, amorphous CEL exhibited FTIR band shifts for those of amorphous form at ambient temperature to those of crystalline form at higher temperatures.

As illustrated in Figure 4, the *N*-H vibration band shifted from wave number positions characteristic of amorphous form to those of crystalline form over the temperature scale studied. At 30°C, a broad band at 3,266 cm^{-1} was observed, whereas the doublet, characteristic of crystalline form, was gained at 80°C. This marks the onset of crystallization event for amorphous CEL. The disparity of crystallization temperatures between DSC and FTIR analysis could be attributable to the presence of an inert atmosphere in the former technique, the absence of which in the latter might have facilitated early crystallization. The position of the low wave number *N*-H band decreased with increase in temperature until T_g, after which it was constant. On the other hand, the high wave number *N*-H band for doublet representing the $-NH_2$ group appeared after the crystallization event, thus signifying the alteration of sites of molecular interaction on the reversal of the crystalline phase from the amorphous one. The position of this band increased continuously with increase in temperature, because of the increase in intermolecular distances on heating. After the melting event at 160°C, both the *N*-H bands showed a sudden increase in band positions, signifying a lack of molecular arrangement in liquid state.

The position of S = O asymmetric stretching vibration band (Figure 4) for amorphous CEL moved continuously to a higher wave number until 80°C, followed by a plateau phase, and a decrease after 150°C, indicating the greater H-bonding of the −S = O group in the molten state. At and above T_g, a marked jump in S = O band position was observed, postulating the sudden gain of molecular mobility in this region[25] conducive to alterations in molecular interactions. Thus, as postulated by FTIR spectral shifts, the temperature-induced phase transformation from amorphous to crystalline state involves the reallocation of molecular interactions.

Effect of Humidity

Water acts as a potential plasticizer that increases the free volume conducive to greater molecular motions favoring devitrification. Storage of amorphous CEL at 25°C and a range of humidity conditions (0%, 35%, 60%, and 80% RH) was found[10] to result in complete devitrification. Storage at high humidities resulted in 100% crystallization in <3 days, whereas 0% RH could sustain the crystallization by allowing 80% crystallization in 75 days. Thus, exposure to humidity favored crystallization of amorphous CEL.

Apart from processing and storage, amorphous systems are exposed primarily to an aqueous environment during dissolution. A rapid rate of devitrification can lead to quick loss of solubility advantage. Amorphous CEL showed higher aqueous solubility than its crystalline form,[7] because of minimal energy required by randomly arranged molecules in an amorphous state for dissolution. A peak in solubility in initial time period (5 minutes) was followed by a decrease to plateau level (after 30 minutes), indicating phase transformation. The drug solubility in the plateau phase was similar to the equilibrium solubility of crystalline CEL. Thus, the initial phase of concentration-time profile

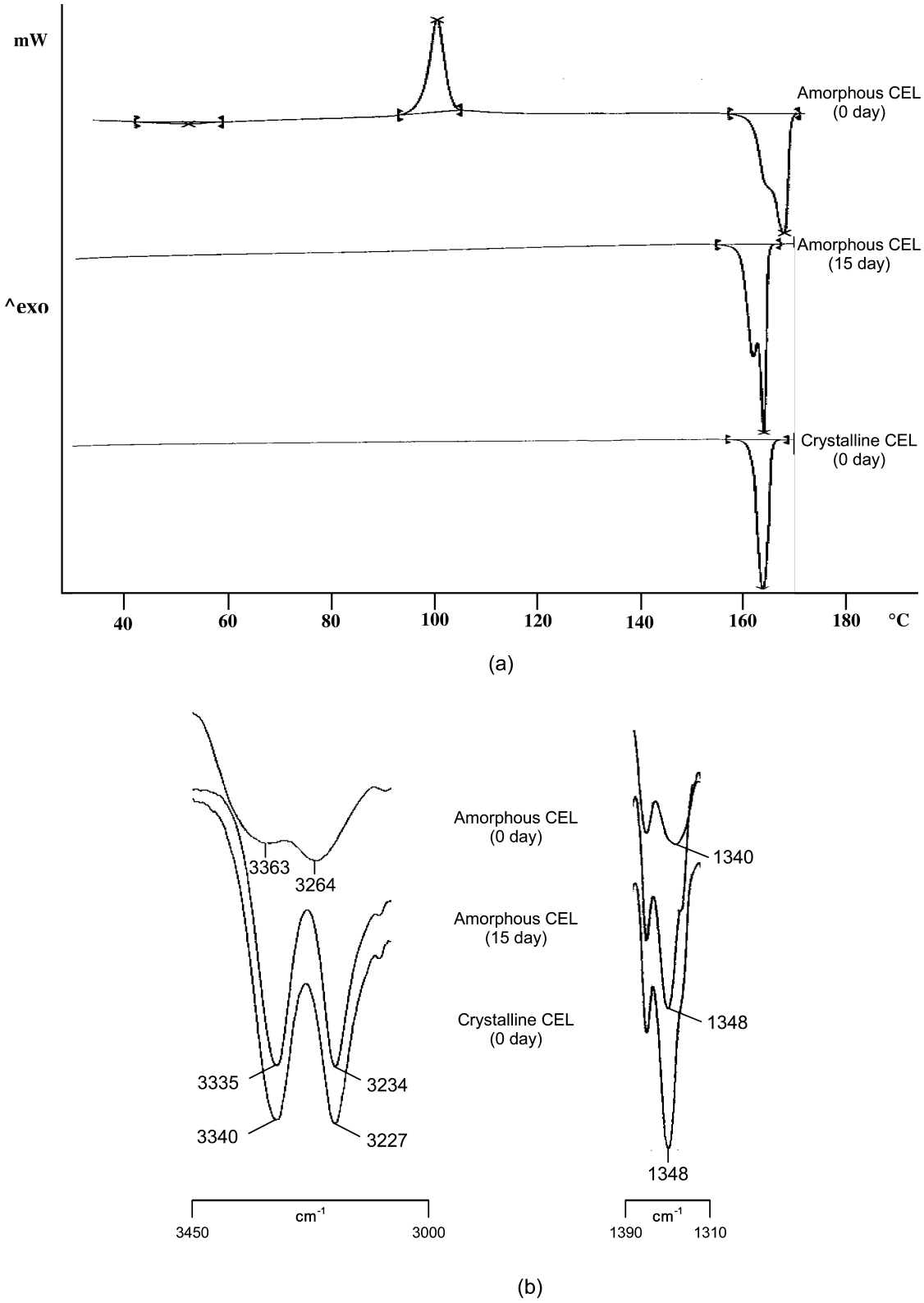

Figure 5. Devitrification of amorphous CEL after exposure to accelerated stability storage conditions (40°C/75% RH), as analyzed by (a) DSC and (b) FTIR spectroscopy.

was dissolution dominated until the highest possible level of supersaturation was reached, that is, the peak, whereas the second phase of the profile was dominated by a transition back to a more thermodynamically stable form, shown by a decline from the peak value. This transition event was also visually observed for amorphous CEL under polarized light microscope, wherein the amorphous sample devitrified immediately on the addition of water.

Effect of Thermal Stress and Humidity

Exposure of amorphous CEL, placed in open glass vials, to International Conference on Harmonization-specified accelerated stability storage condition of 40°C/75% RH in a stability chamber (KBF 720, WTC Binder, Tuttlingen, Germany) resulted in complete reversion into its crystalline form, when tested after 15 days. The DSC analysis (Figure 5A) of aged sample showed a single endotherm (T_m = 164.4°C, ΔH_m = 88.9 J/g), characteristic of melting for the crystalline form. The absence of glass transition and crystallization events confirmed the complete devitrification of amorphous sample. This is a result of water-induced plasticization[10] and greater mobility of CEL molecules at these stressed storage conditions that enhanced the rate and extent of crystallization. Similarly, the FTIR analysis (Figure 5B) of an aged sample showed recovery of sharp doublet for *N*-H stretching and band position for S = O asymmetric stretching characteristic of crystalline CEL, which were lost because of amorphization. Thus, the extensive relaxation of glassy sample under these storage conditions proceeded to complete crystallization, forming a stable and ordered lattice network.

Significance of Effect of Processing Stress on Devitrification of Amorphous Solid

The disordered molecular arrangement in amorphous form contributes excess properties (ie, enthalpy, entropy, and free energy),[26] which act as a constant driving force for loss of energy and regain of order by reverting to the thermodynamically stable crystalline form. The dissipation of this energy could be enhanced to a variable extent in the presence of different stress-inducers. Manufacturing of a solid dosage form involves various unit operations, like size reduction (mechanical and thermal stress), drying (thermal stress), blending (mechanical stress), granulation (mechanical and humidity stress), compression (mechanical and thermal stress), coating (thermal and humidity stress), and so forth, which can provide sufficient inputs for reducing the energy gap between the metastable amorphous and stable crystalline form.

The presently investigated behavior of amorphous CEL in the presence of these processing stresses would allow for adoption of suitable measures in the designing of amorphous systems that can be advantageously used. To eliminate the small crystalline fractions retained during preparation of amorphous CEL, inclusion of high T_g additives can provide benefit in terms of reduction of molecular motions within the experimental time frame. This goal had been achieved with the use of poly(vinyl pyrrolidone),[10] which provided stability to amorphous CEL during storage, as well as dissolution.

CONCLUSION

The devitrification process of an amorphous solid, represented by structural relaxation, subsequent nucleation, and crystal growth, depends on the energy difference between the 2 states. Temperature and humidity played a significant role in reducing the energy gap between glassy and crystalline phases of CEL and promoted devitrification.

ACKNOWLEDGMENTS

Glynn Van-de-Velde (Triton Technology Ltd, Nottinghamshire, United Kingdom) and Sandipan Guha (S.G. Instruments Pvt Ltd, New Delhi, India) are gratefully acknowledged for DMTA studies.

REFERENCES

1. Kaushal AM, Gupta P, Bansal AK. Amorphous drug delivery systems: Molecular aspects, design and performance. *Crit Rev Ther Drug Carrier Syst.* 2004;21:133-193.

2. Tang XC, Pikal MJ, Taylor LS. A spectroscopic investigation of hydrogen bond patterns in crystalline and amorphous phases in dihydropyridine calcium channel blockers. *Pharm Res.* 2002;19:477-483.

3. Brittain HG. Effects of mechanical processing on phase composition. *J Pharm Sci.* 2002;91:1573-1580.

4. York P. Solid-state properties of powders in the formulation and processing of solid dosage forms. *Int J Pharm.* 1983;14:1-28.

5. Sjokvist E, Nystrom C. Physicochemical aspects of drug release. XI. Tableting properties of solid dispersions, using xylitol as carrier material. *Int J Pharm.* 1991;67:139-153.

6. Hancock BC, Carlson GT, Ladipo DD, Langdon BA, Mullarney MP. Comparison of the mechanical properties of the crystalline and amorphous forms of a drug substance. *Int J Pharm.* 2002;241:73-85.

7. Chawla G, Gupta P, Thilagavathi R, Chakraborti AK, Bansal AK. Characterization of solid-state forms of celecoxib. *Eur J Pharm Sci.* 2003;20:305-317.

8. Gupta P, Chawla G, Bansal AK. Physical stability and solubility advantage from amorphous celecoxib: The role of thermodynamic quantities and molecular mobility. *Mol Pharm.* 2004;1:406-413.

9. Kakumanu VK, Bansal AK. Enthalpy relaxation studies of celecoxib amorphous mixtures. *Pharm Res.* 2002;19:1873-1878.

10. Gupta P, Kakumanu VK, Bansal AK. Stability and solubility of celecoxib-PVP amorphous dispersions: A molecular perspective. *Pharm Res.* 2004;21:1762-1769.

11. Kararli TT, Hurlbut JB, Needham TE. Glass-rubber transitions of cellulosic polymers by dynamic mechanical analysis. *J Pharm Sci.* 1990;79:845-848.

12. Craig DQM, Johnson FA. Pharmaceutical applications of dynamic mechanical thermal analysis. *Thermochim Acta.* 1995;248:97-115.

13. Ford JL, Timmins P. Pharmaceutical Thermal Analysis: Techniques and Applications. Chichester, UK: Ellis Horwood Ltd; 1989.

14. Riesen R, Schawe J. The glass transition temperature measured by different TA techniques. Part 1: Overview. *User Com Mettler Toledo.* 2003;1:1-4.

15. Neilson LE. Mechanical tests and polymer transitions; Elastic moduli; and Dynamic mechanical properties. In: *Mechanical Properties of Polymers and Composites*, New York: Marcel Dekker, 1974;11-17,47-52,139-231.

16. Riesen R, Schawe J. The glass transition temperature measured by different TA techniques. Part 2: Determination of glass transition temperatures. *User Com Mettler Toledo.* 2003;2:1-5.

17. Foreman J, Sauerbrunn SR, Marcozzi CL. Exploring the sensitivity of thermal analysis techniques to the glass transition. TA Instruments: Thermal Analysis & Rheology, Application note number TA-082B, http://www.tainst.com.

18. Omelczuk MO, McGinity JW. The influence of polymer glass transition temperature and molecular weight on drug release from tablets containing poly(DL-lactic acid). *Pharm Res.* 1992;9:26-32.

19. Miller DP, Pablo JJ, Corti H. Thermophysical properties of trehalose and its concentrated aqueous solutions. *Pharm Res.* 1997;14:578-590.

20. Hodge IM. Enthalpy relaxation and recovery in amorphous materials. *J Non-Cryst Solids.* 1994;169:211-266.

21. Ferro LJ, Miyake PJ. Polymorphic crystalline forms of celecoxib. 2001;WO 01/42222 A1.

22. Ostwald W. Studien uber die bildung und umwandlung fester korper. *Zieitschrigt Fur Physikalische Chemi.* 1897;22:289-330.

23. Slootmaekers B, Desseyn HO. Characterization of inter- and intramolecular hydrogen bonding in the solid state using variable-temperature IR spectroscopy. *Appl Spectrosc.* 1991;45:118-120.

24. Ediger MD, Angell CA, Nagel SR. Supercooled liquids and glasses. *J Phys Chem.* 1996;100:13200-13212.

25. Hancock BC, Shamblin SL. Molecular mobility of amorphous pharmaceuticals determined using differential scanning calorimetry. *Thermochim Acta.* 2001;380:95-107.

26. Yu L. Amorphous pharmaceutical solids: Preparation, characterization and stabilization. *Adv Drug Del Rev.* 2001;48:27-42.